ISSN(Online) : 2319-8753
ISSN (Print) : 2347-6710

International Journal of Innovative Research in Science, Engineering and Technology

(An ISO 3297: 2007 Certified Organization)

Vol. 5, Issue 4, April 2016

Design, Analysis and Implementation of Solar Power Optimizer for DC Distribution System

Dr.V.Balakrishna Reddy

Professor, Department of EEE, Vijay Rural Engineering College, Nizam Bad, Telangana, India

ABSTRACT: This paper proposes a high step-up solar power optimizer (SPO) that efficiently harvests maximum energy from a photovoltaic (PV) panel then outputs energy to a dc-micro grid. Its structure integrates coupled inductor and switched capacitor technologies to realize high step-up voltage gain. The leakage inductance energy of the coupled inductor can be recycled to reduce voltage stress and power losses. A low voltage rating and low-conduction resistance switch improves system efficiency by employing the incremental conductance method for the maximum power point tracking (MPPT) algorithm. Because of its high tracking accuracy, the method is widely used in the energy harvesting of PV systems. The simulation is carried over by the MATLAB-SIMULINK software. The hardware design is implemented by PIC16F877A controller circuit.

KEYWORDS: MPPT,PV Bus, SPO,CCM,V_{in},V_o,F_s

I. INTRODUCTION

GENERAL

A power optimizer is a DC to DC converter technology developed to maximize the energy harvest from solar photovoltaic or wind turbine systems. They do this by individually tuning the performance of the panel or wind turbine through maximum power point tracking, and optionally tuning the output to match the performance of the string inverter. Power optimizers are especially useful when the performance of the power generating components in a distributed system will vary widely, differences in equipment, shading of light or wind, or being installed facing different directions or widely separated locations. Power optimizers for solar applications, can be similar to microinverters, in that both systems attempt to isolate individual panels in order to improve overall system performance. A microinverter essentially combines a power optimizer with a small inverter in a single case that is used on every panel, while the power optimizer leaves the inverter in a separate box and uses only one inverter for the entire array. The claimed advantage to this "hybrid" approach is lower overall system costs, avoiding the distribution of electronics.

SCOPE OF THE PROJECT

The proposed converter has the following features: 1) its voltage conversion ratio is efficiently increased by using the switched capacitor and coupled inductor techniques; 2) the leakage inductance energy of the coupled inductor can be recycled to increase efficiency, and the voltage spike on the active switch is restrained; 3) the floating active switch isolates the PV panel's energy during non operating conditions, thereby preventing any potential electric hazard to humans or facilities. The MPPT control algorithm exhibits high-tracking efficiency; hence, it is widely used in the energy harvesting of PV systems.

EXISTING SYSTEM

A conventional PV generation system is either a single- or a multistring PV array that is connected to one or several central PV inverters. Numerous series-connected PV modules are connected in the PV array to achieve the DC link voltage that is high enough to be connected to electricity through the DCAC inverter. However, the power reduction that is caused by the shadow effect is an inevitable problem in a centralized PV system.

ISSN(Online) : 2319-8753
ISSN (Print) : 2347-6710

International Journal of Innovative Research in Science, Engineering and Technology

(An ISO 3297: 2007 Certified Organization)

Vol. 5, Issue 4, April 2016

EXISTING SYSTEMS TECHNIQUE:

In the traditional grid-connected PV inverters, either a line frequency or a high-frequency transformer is utilized to provide a galvanic isolation between the grid and the PV panels. For a typical PV array, the output voltage is relatively low, and a high voltage gain is obligatory to realize the grid-connected function.

PROPOSED SYSTEM

A solar power optimizer (SPO) was developed as an alternative to maximize energy harvest from each individual PV module. An SPO is used as a dc–dc converter with maximum power point tracking (MPPT), which increases PV panel voltage to optimum voltage levels for a dc microgrid connection. The SPO attempts to improve the use of distributed renewable resources and lower system cost. It may also potentially improve the efficiency of PV systems, has an antishadow effect, and can monitor the status of PV modules.

PROPOSED SYSTEM TECHNIQUE

The proposed SPO's configuration is based on a high step-up dc–dc converter with an MPPT control circuit. The converter includes a floating active switch S and a coupled inductor *T*1 with primary winding *N*1, which is similar to the input inductor of a conventional boost converter capacitor *C*1, and diode *D*1 recycle leakage inductance energy from *N*1. Secondary winding *N*2 is connected to another pair of capacitors, *C*2 and *C*3, and to diodes *D*2 and *D*3. Rectifier diode *D*4 connects to output capacitor *Co* and load *R*. The duty ratio is modulated by the MPPT algorithm, which uses the incremental conductance method is employed in the proposed SPO.

ADVANTAGES OF PROPOSED TECHNIQUE

- Improve voltage level.
- Recycling the leakage inductance energy.
- Reduce the voltage stress on the switch.
- Improved power capacity.

II. CIRCUIT DIAGRAM

Circuit Diagram Proposed

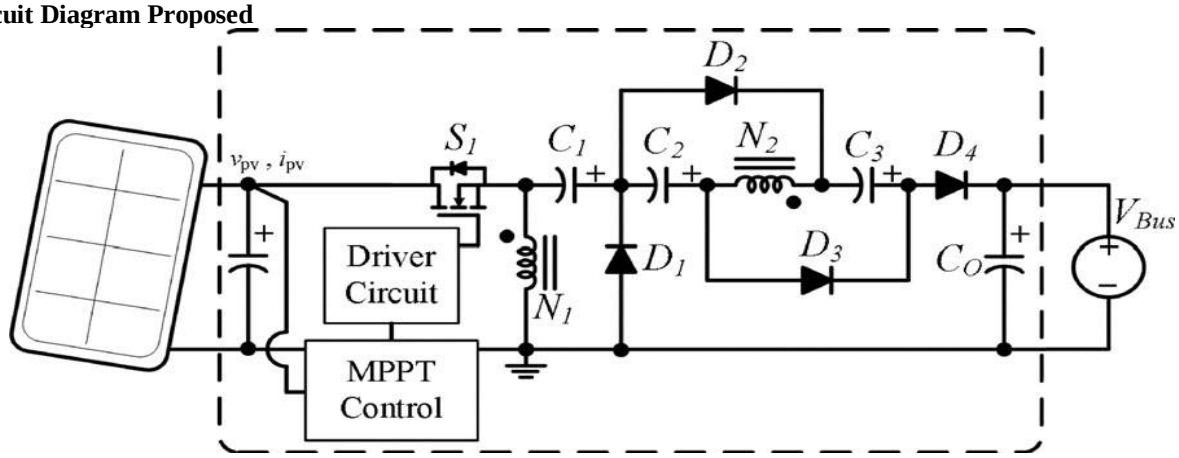

Fig.1

The proposed SPO is shown in Fig. 1; its configuration is based on a high step-up dc–dc converter with an MPPT control circuit. The converter includes a floating active switch S and a coupled inductor *T*1 with primary winding *N*1 , which is similar to the input inductor of a conventional boost converter capacitor *C*1 , and diode *D*1 recycle leakage inductance energy from *N*1 . Secondary winding *N*2 is connected to another pair of capacitors, *C*2 and *C*3 , and to diodes *D*2 and *D*3 . Rectifier diode *D*4 connects to output capacitor *Co* and load *R*. The duty ratio is

ISSN(Online) : 2319-8753
ISSN (Print) : 2347-6710

International Journal of Innovative Research in Science, Engineering and Technology

(An ISO 3297: 2007 Certified Organization)

Vol. 5, Issue 4, April 2016

modulated by the MPPT algorithm, which uses the perturb and observer method that is employed in the proposed SPO. It detects PV module voltage *V*pv and current *I*pv to determine the increase and decrease in the duty cycle of the dc converter. Therefore, the MPP can be obtained by comparing instantaneous conductance *I/V* and incremental conductance *dI/dV*.

The proposed converter has the following features:

1) its voltage conversion ratio is efficiently increased by using the switched capacitor and coupled inductor techniques;

2) The leakage inductance energy of the coupled inductor can be recycled to increase efficiency, and the voltage spike on the active switch is restrained;

3) The floating active switch isolates the PV panel's energy during non operating conditions, thereby preventing any potential electric hazard to humans or facilities. The MPPT control algorithm exhibits high-tracking efficiency;

Operation Modes

The operating principles for continuous conduction mode (CCM) and discontinuous conduction mode (DCM) are presented in detail and shown in schematic form in **Fig.1**.

A. CCM OPERATION

The CCM operating modes are described as follows.

Mode I [t0 , t1]: During this interval, switch *S* and diodes *D*2 and *D*3 are conducted; diodes *D*1 and *D*4 are turned OFF. The current flow path is shown in Fig.(a). Magnetizing inductor *Lm* continues to release energy to capacitors *C*2 and *C*3 through secondary winding*N*2 of coupled inductor *T*1 . Leakage inductance *Lk* 1 denotes the stored energy from source energy *V*in . The energy that is stored in capacitor *Co* is constantly discharged to load *R*. This mode ends when increasing *iLk*1 is equal to decreasing *iLm* at *t* = *t*1.

$$v_{Lm} = V_{\text{in}}$$

$$\Delta i_{Lm} = \frac{V_{\text{in}}}{L_m}(t_1 - t_0).$$

$$v_{Lm} = \frac{V_o - V_{\text{in}} - V_{c1} - V_{c2} - V_{c3}}{n}$$

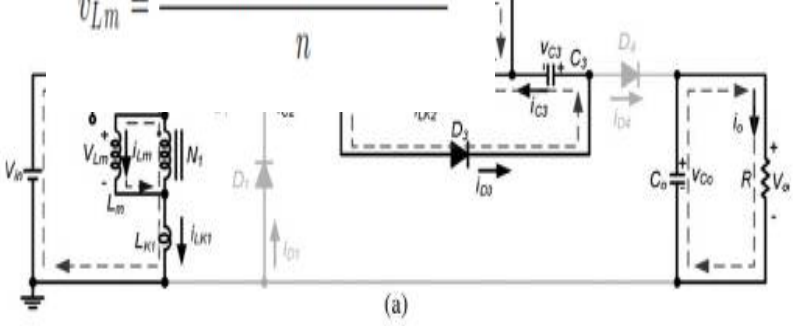

Mode II [t1 , t2]: During this interval, switch *S* and diode *D*4 are conducted. Source energy *V*in is serially connected to *C*1, *C*2 , and *C*3 , and secondary winding *N*2 ; *Lk*2 discharges the energy that is stored in charge output capacitor *Co* and loads *R*. Meanwhile, magnetizing inductor *Lm* also receives energy from *V*in . The current flow path is shown in Fig.(b). This mode ends when switch S is turned OFF at *t* = *t*2.

ISSN(Online) : 2319-8753
ISSN (Print) : 2347-6710

International Journal of Innovative Research in Science, Engineering and Technology

(An ISO 3297: 2007 Certified Organization)

Vol. 5, Issue 4, April 2016

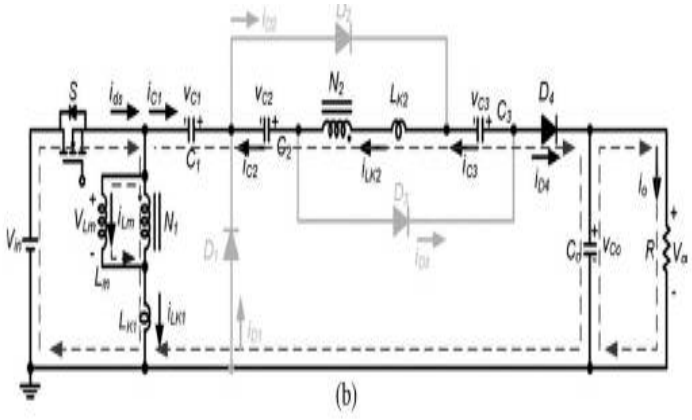

(b)

Mode III [t2 , t3]: During this transition interval, switch *S* and diodes *D*2 and *D*3 are turned OFF, and diodes *D*1 and *D*4 are conducted. The current flow path is shown in Fig.(c). The energy stored in leakage inductance *Lk* 1 instantly flows through the diode *D*1 to charge capacitor *C*1 . The energy is released to magnetizing inductor *Lm* through coupled inductor *T*1 , which is serially connected to *C*1, *C*2 , and *C*3 , and secondary winding *N*2 ; *Lk*2 discharges the energy that is stored in charge output capacitor *Co* and loads *R*. This mode ends when decreasing *iLk*1 is equal to increasing *iLm* at *t* = *t*3.

$$v_{Lm} = -V_{c1}$$

$$\Delta i_{Lm} = \frac{-V_{c1}}{L_m} \cdot (t_3 - t_2).$$

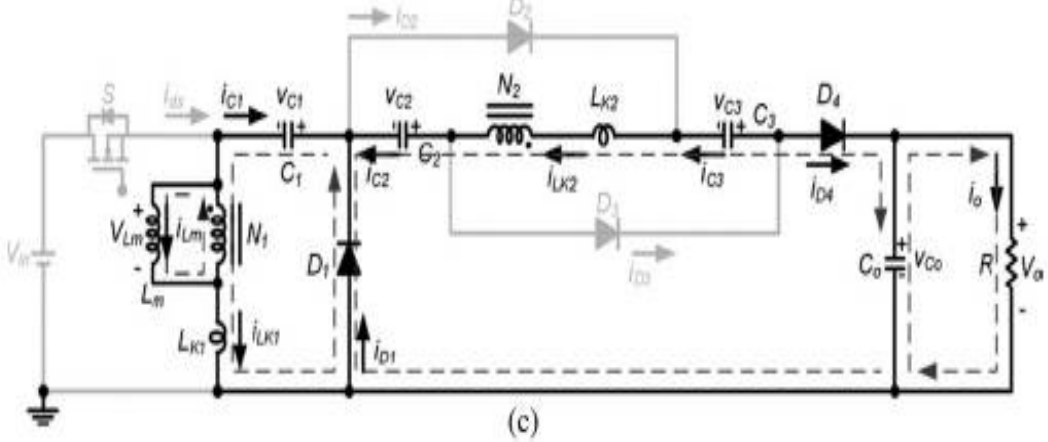

(c)

Mode IV [t3 , t4]: During this interval, switch *S* and diode *D*4 are turned OFF, and diodes *D*1,*D*2 , and *D*3 are conducted. The current flow path is shown in Fig.(d). Leakage inductance *Lk* 1 continues to release energy to charge capacitor *C*1 through diode *D*1 . Magnetizing inductor *Lm* through coupled inductor *T*1 transfers energy to capacitors *C*2 and *C*3 . The energy that is stored in capacitor *CO* is constantly discharged to load *R*. This mode ends when decreasing *iLk*1 is zero at *t* = *t*4.

$$v_{Lm} = -V_{c1}$$

$$\Delta i_{Lm} = \frac{-V_{c1}}{L_m} \cdot (t_4 - t_3).$$

ISSN(Online) : 2319-8753
ISSN (Print) : 2347-6710

International Journal of Innovative Research in Science, Engineering and Technology

(An ISO 3297: 2007 Certified Organization)

Vol. 5, Issue 4, April 2016

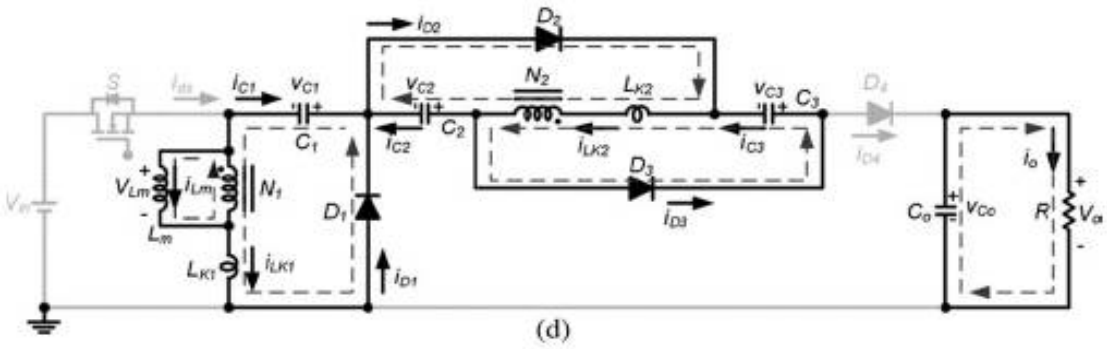

(d)

Mode V [t4 , t5]: During this interval, diodes *D*2 and *D*3 are conducted. The current flow path is shown in Fig.(e). Magnetizing inductor *Lm* constantly transfers energy to secondary winding *N*2 , and charges capacitors *C*2 and *C*3 . The energy that is stored in capacitor *CO* is constantly discharged to load *R*. This mode ends when switch S is turned ON at the beginning of the next switching period.

$$v_{Lm} = \frac{-V_{c2}}{n} = \frac{-V_{c3}}{n}$$

$$\Delta i_{Lm} = \frac{-V_{c2}}{n \cdot L_m} \cdot (t_5 - t_4) = \frac{-V_{c3}}{n \cdot L_m} \cdot (t_5 - t_4).$$

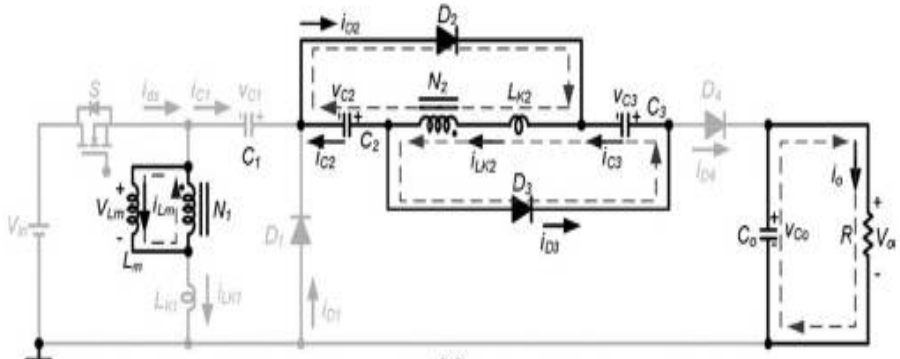

(e)

B. DCM OPERATION

Mode I [t0 , t1]: During this interval, switch *S* and *D*4 are conducted, and diodes *D*1,*D*2 , and *D*3 are turned OFF. The current flowpath is shown in Fig. 6(a).Magnetizing inductor*Lm* with leakage inductance *Lk* 1 stores energy from source energy *V*in . Meanwhile, source energy *V*in is also serially connected to capacitors *C*1, *C*2 , and *C*3 , and secondary winding *N*2 to charge capacitor *Co* and load *R*. This mode ends when switch *S* is turned OFF at *t* = *t*1.

$$v_{Lm} = V_{\text{in}} = \frac{V_o - V_{\text{in}} - V_{c1} - V_{c2} - V_{c3}}{n}$$

ISSN(Online) : 2319-8753
ISSN (Print) : 2347-6710

International Journal of Innovative Research in Science, Engineering and Technology

(An ISO 3297: 2007 Certified Organization)

Vol. 5, Issue 4, April 2016

$$\Delta i_{Lm} = \frac{V_{in}}{L_m} \cdot (t_1 - t_0) = \frac{V_o - V_{in} - V_{c1} - V_{c2} - V_{c3}}{n \cdot L_m} \cdot (t_1 - t_0).$$

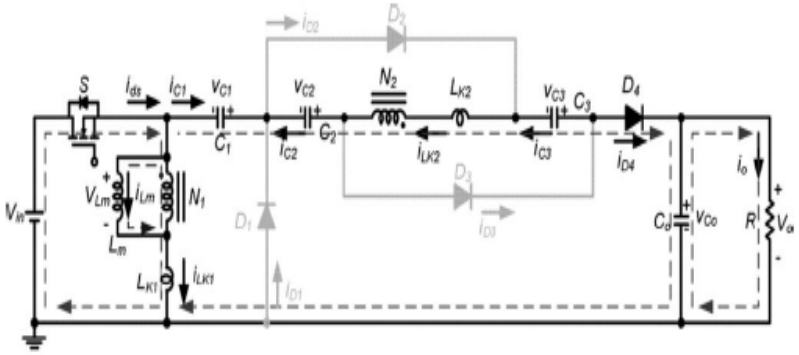

Fig: f

Mode II [t1 , t2]: During this transition interval, switch *S* and diodes *D*2 and *D*3 are turned OFF, and diodes *D*1 and *D*4 are conducted. The current flow path is shown in Fig. 6(b). The energy stored in leakage inductance *Lk* 1 instantly flows through the diode*D*1 to charge capacitor *C*1 ; this energy is also released to magnetizing inductor *Lm* through the coupled inductor *T*1 series that is connected to *C*1, *C*2 , and *C*3 , secondary winding *N*2 , and *Lk*2 to charge output capacitor *Co* and load *R*. This mode ends when decreasing *iD*4 is zero at *t* = *t*2.

$$v_{Lm} = -V_{c1}$$

$$\Delta i_{Lm} = \frac{-V_{c1}}{n \cdot L_m} \cdot (t_2 - t_1).$$

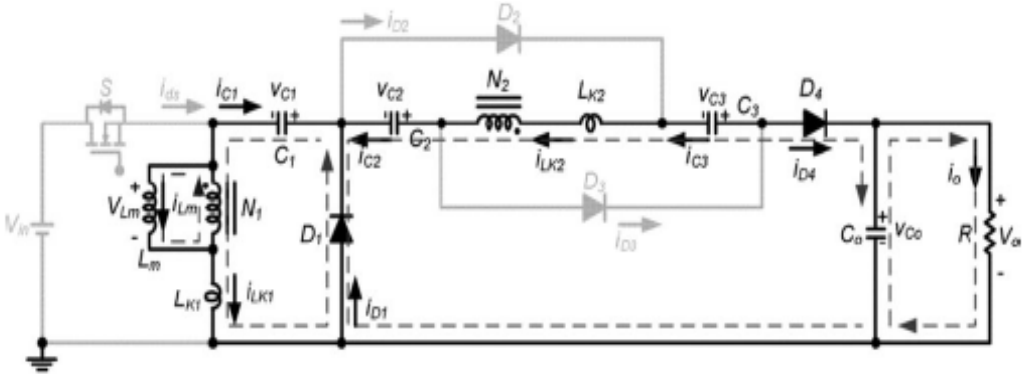

Fig: g

Mode III [t2 , t3]: During this transition interval, switch *S* and diode *D*4 are turned OFF, and diodes *D*1,*D*2 , and *D*3 are conducted. The current flow path is shown in Fig. 6(c). Leakage inductance *Lk* 1 continues to release energy to charge capacitor *C*1 through diode *D*1 . agnetizing inductor *Lm* transfers energy to capacitors *C*2 and *C*3 through coupled inductor *T*1. The energy stored in capacitor *Co* is constantly discharged to load *R*. This mode ends when decreasing *iLk*1 is zero at *t* = *t*3.

ISSN(Online) : 2319-8753
ISSN (Print) : 2347-6710

International Journal of Innovative Research in Science, Engineering and Technology

(An ISO 3297: 2007 Certified Organization)

Vol. 5, Issue 4, April 2016

$$v_{Lm} = -V_{c1} = \frac{-V_{c2}}{n} = \frac{-V_{c3}}{n}$$

$$\Delta i_{Lm} = \frac{-V_{c1}}{n \cdot L_m} \cdot (t_3 - t_2) = \frac{-V_{c2}}{n \cdot L_m} \cdot (t_3 - t_2)$$

$$= \frac{-V_{c3}}{n \cdot L_m} \cdot (t_3 - t_2).$$

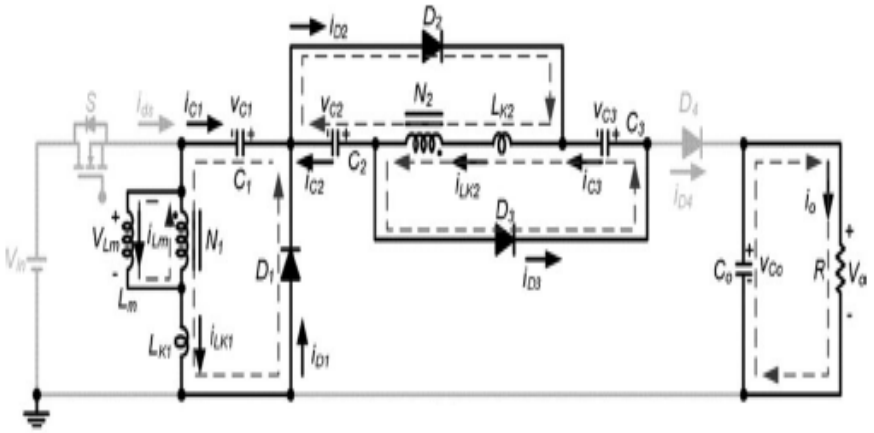

Fig: h

Mode IV [t3 , t4]: During this interval, switch *S*, diodes *D*1 and *D*4 are turned OFF, and diodes *D*2 and *D*3 are conducted. The current flow path is shown in Fig. 6(d).Magnetizing inductor *Lm* constantly transfers energy to secondary winding *N*2 and charges capacitors *C*2 and *C*3 . The energy that is stored in capacitor *Co* is constantly discharged to load *R*. This mode ends
when decreasing *iLm* is zero at *t* = *t*4.

$$v_{Lm} = \frac{-V_{c2}}{n} = \frac{-V_{c3}}{n}$$

$$\Delta i_{Lm} = \frac{-V_{c2}}{n \cdot L_m} \cdot (t_5 - t_4) = \frac{-V_{c3}}{n \cdot L_m} \cdot (t_4 - t_3).$$

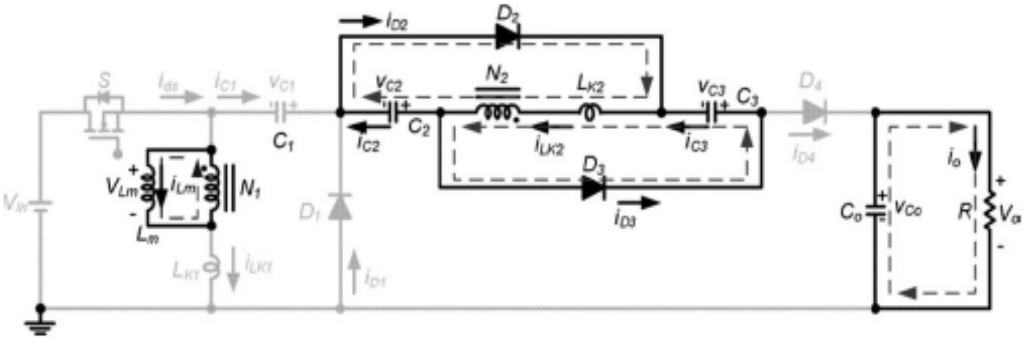

Fig: i

ISSN(Online) : 2319-8753
ISSN (Print) : 2347-6710

International Journal of Innovative Research in Science, Engineering and Technology

(An ISO 3297: 2007 Certified Organization)

Vol. 5, Issue 4, April 2016

Mode V [t4 , t5]: During this interval, the switch and all the diodes are turned OFF. The current flow path is shown in Fig. 6(e). The energy that is stored in capacitor *CO* is constantly
discharged to load *R*. This mode ends when switch S is turned ON at the beginning of the next switching period.

$$v_{Lm} = 0$$
$$\Delta i_{Lm} = 0.$$

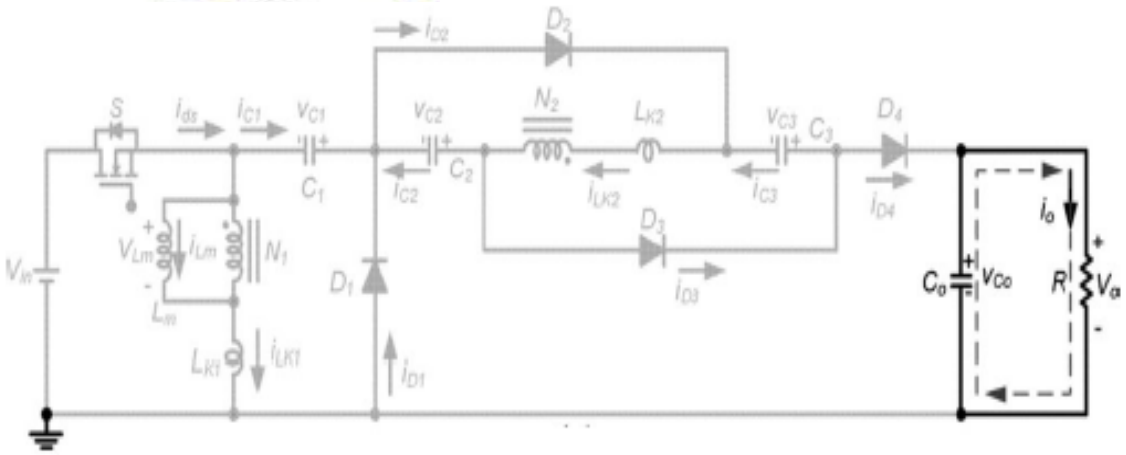

Fig: j

III. SIMULATION RESULTS

TECHNIQUES USED

In the traditional grid-connected PV inverters, either a line frequency or a high-frequency transformer is utilized to provide a galvanic isolation between the grid and the PV panels. For a typical PV array, the output voltage is relatively low, and a high voltage gain is obligatory to realize the grid-connected function.

POWER STAGE DESIGN PARAMETERS

Full PV output power	300 W
Input voltage, V_{in}	20–40 V
Output voltage, V_o	400 V
Switching frequency, f_S	50 kHz

ISSN(Online) : 2319-8753
ISSN (Print) : 2347-6710

International Journal of Innovative Research in Science, Engineering and Technology

(An ISO 3297: 2007 Certified Organization)

Vol. 5, Issue 4, April 2016

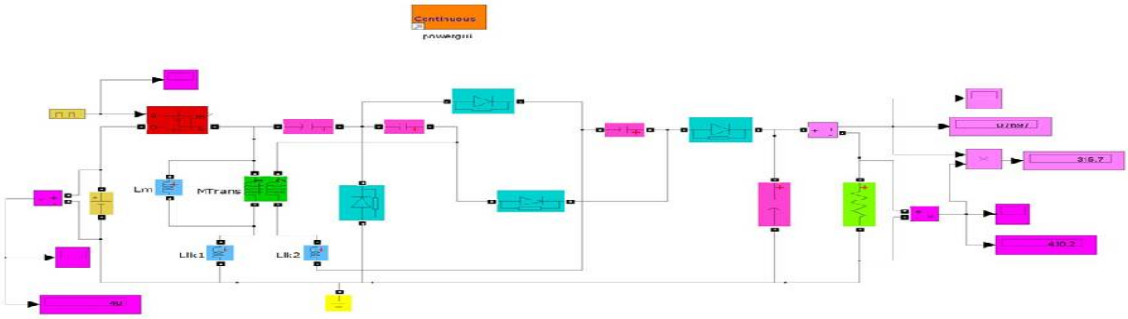

OPEN LOOP CIRCUIT OF SOLAR POWER OPTIMIZER

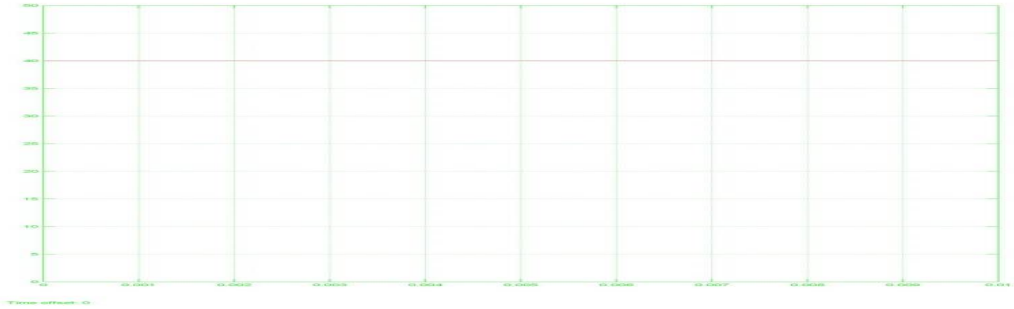

INPUT VOLTAGE WAVEFORM

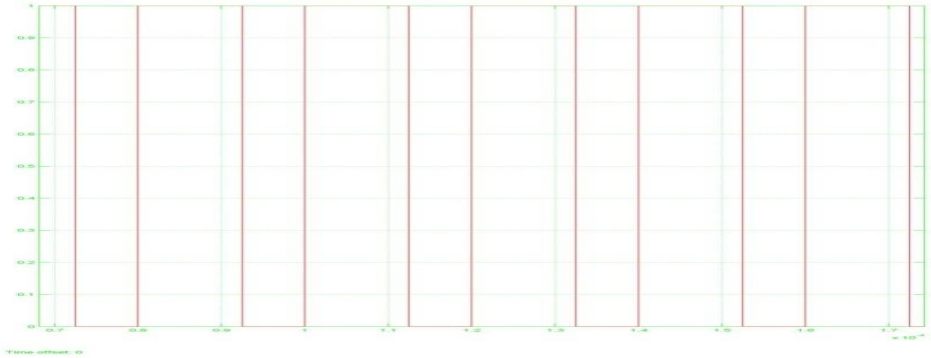

OUTPUT VOLTAGE WAVEFORM

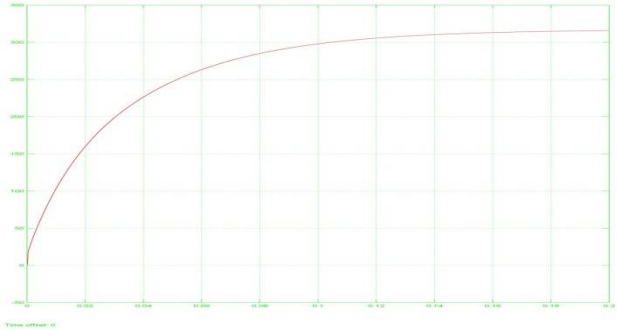

OUTPUT POWER WAVEFORM

ISSN(Online) : 2319-8753
ISSN (Print) : 2347-6710

International Journal of Innovative Research in Science, Engineering and Technology

(An ISO 3297: 2007 Certified Organization)

Vol. 5, Issue 4, April 2016

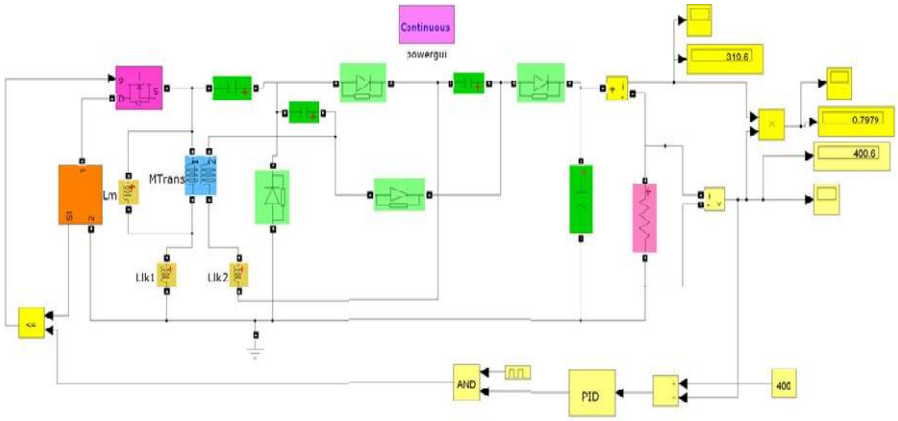

CLOSED LOOP CIRCUIT OF SOLAR POWER OPTIMIZER

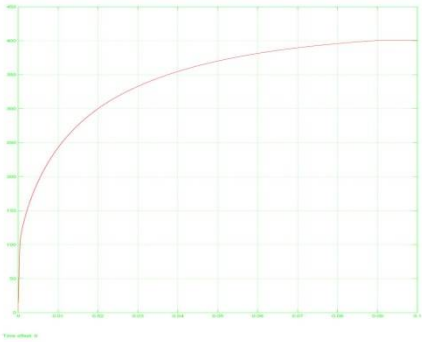

OUTPUT VOLTAGE WAVEFORM

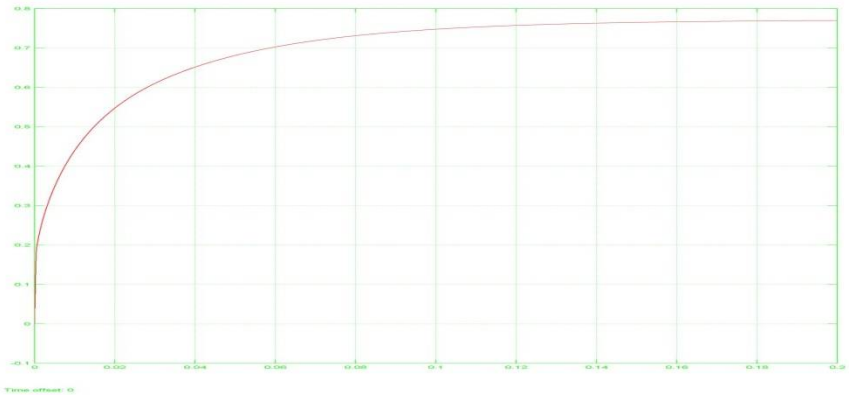

OUTPUT CURRENT WAVEFORM

IV. CONCLUSION

APPLICATIONS

- High voltage application.
- Tele communication.
- Grid tie inverter & stand alone inverter

ISSN(Online) : 2319-8753
ISSN (Print) : 2347-6710

International Journal of Innovative Research in Science, Engineering and Technology

(An ISO 3297: 2007 Certified Organization)

Vol. 5, Issue 4, April 2016

FUTURE SCOPE

The system can be extended for more voltage range. Increase in more voltage range will increases the voltage gain and efficiency of the converter system. The output DC voltage can be inverted and we can use the AC loads also.

REFERENCES

1. W. Yu, J.-S. Lai, H. Qian, and C. Hutchens, "High-efficiency MOSFET inverter with H6-type configuration for photovoltaic non isolated ac-module applications," IEEE Trans. Power Electron., vol. 26, no. 4, pp. 1253–1260, Apr. 2011.
2. L. Gao, R. A. Dougal, S. Liu, and A. P. Iotova, "Parallel-connected solar PV system to address partial and rapidly fluctuating shadow conditions," *IEEE Trans. Ind. Electron.*, vol. 56, no. 5, pp. 1548–1556, May 2009.
3. R. Gules, J. De Pellegrin Pacheco, H. L. Hey, and J. Imhoff, "A maximum power point tracking system with parallel connection for PV stand-alone applications," *IEEE Trans. Ind. Electron.*, vol. 55, no. 7, pp. 2674–2683, Jul. 2008.
4. B. Liu, S. Duan, and T. Cai, "Photovoltaic dc-building-module-based BIPV system: Concept and design considerations," *IEEE Trans. Power Electron.*, vol. 26, no. 5, pp. 1418–1429, May 2011.
5. W. Xiao, N. Ozog, and W. G. Dunford, "Topology study of photovoltaic interface for maximum power point tracking," *IEEE Trans. Ind. Electron.*, vol. 54, no. 3, pp. 1696–1704, Jun. 2007.